Title

The glucocorticoid receptor represses, whereas C/EBPβ can enhance or repress *CYP26A1* transcription.

Journal

iScience, 25(7)

ISSN

2589-0042

Authors

Yoo, Hong Sik
Rodriguez, Adrienne
You, Dongjoo
et al.

Publication Date

2022-07-01

DOI

10.1016/j.isci.2022.104564

Peer reviewed

iScience

CellPress
OPEN ACCESS

Article

The glucocorticoid receptor represses, whereas C/EBPβ can enhance or repress *CYP26A1* transcription

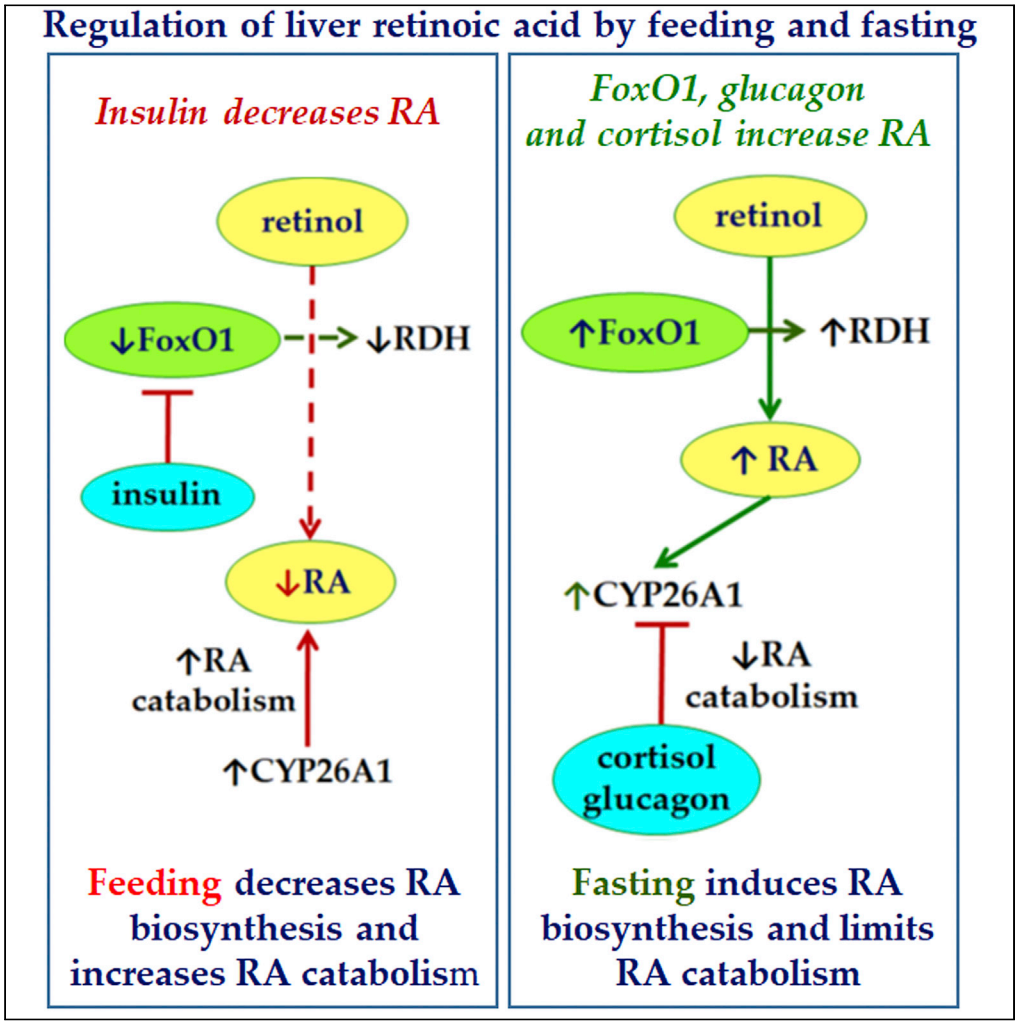

Hong Sik Yoo, Adrienne Rodriguez, Dongjoo You, ..., Jen-Chywan Wang, Sona Kang, Joseph L. Napoli

jna@berkeley.edu

Highlights

Glucocorticoids and glucagon increase liver retinoic acid concentrations during fasting

The glucocorticoid receptor binds to an RAR/RXR coactivation complex to reduce *CYP26A1* transcription

C/EBPβ binding to a major allele of SNP rs2068888 enhances *CYP26A1* transcription

C/EBPβ binding to a minor allele of SNP rs2068888 inhibits *CYP26A1* transcription

Yoo et al., iScience *25*, 104564
July 15, 2022
https://doi.org/10.1016/j.isci.2022.104564

iScience

CellPress
OPEN ACCESS

Article

The glucocorticoid receptor represses, whereas C/EBPβ can enhance or repress *CYP26A1* transcription

Hong Sik Yoo,[1] Adrienne Rodriguez,[1] Dongjoo You,[1] Rebecca A. Lee,[1] Michael A. Cockrum,[1] Jack A. Grimes,[1] Jen-Chywan Wang,[1] Sona Kang,[1] and Joseph L. Napoli[1,2,*]

SUMMARY

Retinoic acid (RA) counters insulin's metabolic actions. Insulin reduces liver RA biosynthesis by exporting FoxO1 from nuclei. RA induces its catabolism, catalyzed by CYP26A1. A CYP26A1 contribution to RA homeostasis with changes in energy status had not been investigated. We found that glucagon, cortisol, and dexamethasone decrease RA-induced *CYP26A1* transcription, thereby reducing RA oxidation during fasting. Interaction between the glucocorticoid receptor and the RAR/RXR coactivation complex suppresses *CYP26A1* expression, increasing RA's elimination half-life. Interaction between CCAAT-enhancer-binding protein beta (C/EBPβ) and the major allele of SNP rs2068888 enhances *CYP26A1* expression; the minor allele restricts the C/EBPβ effect on *CYP26A1*. The major and minor alleles associate with impaired human health or reduction in blood triglycerides, respectively. Thus, regulating *CYP26A1* transcription contributes to adapting RA to coordinate energy availability with metabolism. These results enhance insight into CYP26A1 effects on RA during changes in energy status and glucocorticoid receptor modification of RAR-regulated gene expression.

INTRODUCTION

All-*trans*-retinoic acid (RA) functions as an autacoid essential to diverse biological processes, encompassing embryonic development, intermediary metabolism, spermatogenesis and cell death, and cell proliferation or differentiation (Schug et al., 2007; Pino-Lagos et al., 2010; Noy, 2013; Das et al., 2014; Gewiss et al., 2020; Lin et al., 2020; Wołoszynowska-Fraser et al., 2020). Enzymatic reactions that regulate RA tissue concentrations involve interconversion of retinol and retinal by retinol dehydrogenases and retinal reductases, dehydrogenation of retinal into RA, and catabolism of RA by Cyp26 isozymes (Pennimpede et al., 2010; Billings et al., 2013; Isoherranen and Zhong, 2019; Belyaeva et al., 2019; Napoli, 2020). RA autoregulates its tissue concentrations by inducing retinol esterification, to limit substrate for its biosynthesis, and by Cyp26-catalyzed degradation (White et al., 1996; Ray et al., 1997; Zolfaghari and Ross, 2000; Wolf, 2001; Liu and Gudas, 2005; Ross and Zolfaghari, 2011; Napoli, 2012). Through binding with RA receptors (RAR), RA initiates *CYP26A1* transcription to establish negative feedback (Abu-Abed et al., 1998; Loudig et al., 2005; Yamamoto et al., 2000). The embryonic lethality of *Cyp26a1* knockout mice illustrates the extent of its contribution to maintaining physiological RA concentrations during fetal development (Abu-Abed et al., 2001). Postnatal *Cyp26a1* ablation, however, did not cause persistent histopathological damage of major organs (Zhong et al., 2019). These knockouts were fed a chow diet *ad libitum* with 20 IU vitamin A/g and beta carotene, more than the total 4 IU/g recommended for rodents (Reeves, 1997). Because RA exerts concentration-dependent actions (hormesis), chow diets with copious vitamin A have altered phenotypes of at least three retinoid-related gene knockouts, *Rdh1*, *Rbp4*, and *Crbp2* (Quadro et al., 1999; E et al., 2002; Zhang et al., 2007). Diets copious in vitamin A also impair glucoregulatory mechanisms (Kane et al., 2011; Napoli, 2022), which were not evaluated in the *Cyp26a1* knockout.

RA regulates energy balance by suppressing pre-adipocyte differentiation into mature white adipocytes (Schwarz et al., 1997; Berry et al., 2012). Ablation of the retinol dehydrogenase *Rdh1* leads to adiposity in mice fed a low-fat diet by disrupting brown adipose tissue adaptation to refeeding (Krois et al., 2019). Heterozygote ablation of the retinol dehydrogenase *Rdh10* increases adiposity in mice fed a high-fat diet (Yang et al., 2018; Zhao et al., 2021). *Rdh10*$^{+/-}$ males develop glucose intolerance and insulin

[1]Department of Nutritional Sciences and Toxicology, Graduate Program in Metabolic Biology, The University of California, Berkeley Berkeley, CA 94720, USA

[2]Lead contact

*Correspondence: jna@berkeley.edu

https://doi.org/10.1016/j.isci.2022.104564

resistance and have dysfunctional mitochondria in muscle. *Rdh10*$^{+/-}$ females undergo extensive adipocyte formation in bone marrow but have improved muscle mitochondria function. These data illustrate the sexually dimorphic effects of RA over energy metabolism.

RA also regulates energy balance indirectly by specifying pancreatic endocrine cell fate, with effects on development of α, β, and δ cells (Martín et al., 2005; Kane et al., 2010; Lorberbaum et al., 2020). Cyp26a1 contributes to RA regulation of pancreatic development by limiting differentiation (Kinkel et al., 2009). After development, RA and its isomers regulate glycemia (Miyazaki et al., 2010; Kane et al., 2011; Trasino et al., 2015, 2016). The impact of retinoids on pancreatic development and glucose-stimulated insulin secretion prompted us to question whether insulin regulates RA homeostasis. In fact, energy status regulates RA biosynthesis at the rate-limiting step, catalyzed by retinol dehydrogenases (Obrochta et al., 2015). Refeeding mice decreases *Rdh1* and *Rdh10* mRNA in the liver, relative to fasted mice, which decrease RA. Insulin causes the decrease by eliminating FoxO1 from nuclei, which reduces *Rdh* transcription and destabilizes *Rdh* mRNA. These data reveal mechanisms for regulating the opposing effects of RA and insulin on gluconeogenesis and lipid metabolism and suggest interaction between RA homeostasis and insulin-signaling-related diseases, such as type II diabetes (Berry and Noy, 2009; Cione et al., 2016).

We considered the contribution of CYP26A1 to liver RA concentrations during fasting and re-feeding because it serves as a major contributor to liver RA catabolism (Thatcher and Isoherranen, 2009). Here we report that *CYP26A1* mRNA decreases during fasting relative to the refed state. Contrary to expectations, insulin did not have a major effect on regulating *CYP26A1*, but glucagon and cortisol limited RA induction of *CYP26A1* mRNA and its catabolic activity. Glucagon and cortisol actions are neither additive nor synergistic. Cortisol acts through the glucocorticoid receptor (GR) and attenuates activity of the RAR-RXR transcription coactivation complex. In contrast, interaction between CCAAT-enhancer-binding protein beta (C/EBPβ) and the major allele of SNP rs2068888 enhances *CYP26A1* expression. Consequently, hormones secreted during fasting suppress RA catabolism by reducing *CYP26A1* transcription and activity, thereby contributing to increasing the RA concentration relative to refeeding. These data enhance insight into regulation of RA concentrations during transition between feeding and fasting, by revealing mechanisms of *CYP26A1* regulation during adaptation to changes in energy balance in mice fed recommended amounts of dietary vitamin A.

RESULTS

Glucocorticoids and glucagon down-regulate *CYP26A1* transcription

We confirmed a decrease in liver RA after transition from the fasted to the re-fed state (Figure 1A). RA decreases ~45% in males and ~38% in females. At the same time, *Cyp26a1* mRNA increases ~4- to 6-fold in livers of re-fed mice compared to fasted mice (Figure 1B). These data suggest that insulin might upregulate *Cyp26a1* mRNA. An insulin challenge *in vivo*, however, did not increase mouse hepatic *Cyp26a1* mRNA (Figure S1). We then chose the human liver cell line HepG2 to investigate mechanisms of regulation because RA induces *CYP26A1* mRNA in HepG2 cells. HepG2 cells also have been used to characterize the RA response elements (RAREs) that drive *CYP26A1* transcription and the substrate specificity of CYP26A1 (Tay et al., 2010; Zhang et al., 2010). Moreover, HepG2 cells have revealed mechanisms of insulin decreasing *Rdh1* and *Rdh10* transcription (Obrochta et al., 2015). RA (0.5 nM) induced *CYP26A1* mRNA within 1 h, rising ~30-fold in 6 h (Figure 1C). Insulin combined with either low (3 mM) or high (20 mM) glucose did not affect RA-induced *CYP26A1* mRNA in HepG2 cells (Figure S2). We re-directed focus to the fasting-secreted hormones cortisol and glucagon. Cortisol decreased RA-induced *CYP26A1* mRNA by 53% (Figure 1D). Glucagon decreased RA-induced *CYP26A1* mRNA by 37%. Cortisol and glucagon effects were neither additive nor synergistic. The combination caused suppression that averaged the two alone (44%), suggesting both function competitively through a similar mechanism. 8-Br-cAMP had no effect on *CYP26A1* mRNA, suggesting a cAMP-independent mechanism (Figure 1E).

We substituted dexamethasone (Dex) for cortisol. Dex suppressed induction at ~50% regardless of the RA concentration (Figure 1F). As low as 1 nM Dex reduced *CYP26A1* mRNA (Figure 1G). Dex had a more potent effect than cortisol, as expected, because Dex has a lower k_d for the GR (Pratt et al., 1975). The Dex repressive effect also decreased *CYP26A1* enzymatic activity (Figure 1H). The RA concentration decreased more slowly in HepG2 cells treated with RA and Dex compared to cells treated with RA alone. RA had an elimination half-life of 6.7 h in the absence of Dex, which Dex increased to 10.6 h. Dex also suppressed RA-induced *CYP26A1* transcription in primary human hepatocytes Figure 1I).

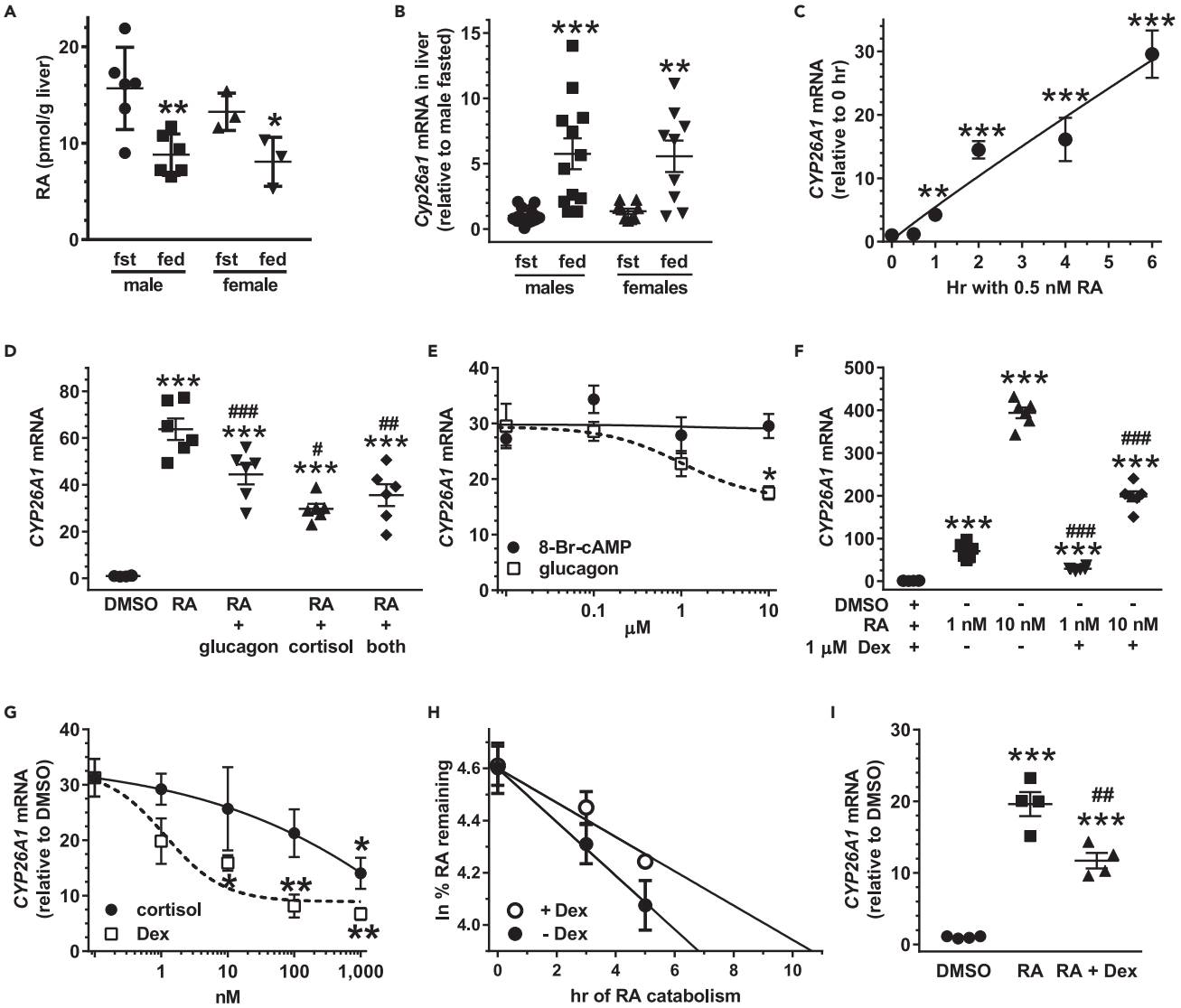

Figure 1. Glucocorticoids and glucagon down-regulate *CYP26A1* transcription

(A) Decrease in liver RA 6 h after onset of refeeding male and female C57Bl/6J mice between 16 h fasted and 16 h fasted followed by 6 h refed (males, n = 6, **p < 0.01 vs fasted; females, n = 3, *p < 0.05 vs fasted).

(B) Comparison of *Cyp26a1* mRNA in livers of male and female C57Bl/6J mice between 16 h fasted and 16 h fasted followed by 6 h re-fed (n = 9-14, **p < 0.01, ***p < 0.001 vs fasted).

(C) Time-course of *CYP26A1* mRNA increase in HepG2 cells induced by 0.5 nM RA (n = 6, **p < 0.01, ***p < 0.001 vs. 0 h).

(D) HepG2 cells were treated 6 h with 0.1% DMSO or 1 nM RA ± 1 μM cortisol, ± 1 μM glucagon, or ± both (n = 6, ***p < 0.001 vs. 0.1% DMSO, #p < 0.05, ##p < 0.01, ###p < 0.001 vs. RA).

(E) HepG2 cells were treated 6 h with 0.1% DMSO or 1 nM RA ± increasing concentrations of glucagon or 8-Br-cAMP (n = 3, *p < 0.05 vs. RA).

(F) HepG2 cells were treated 6 h with 0.1% DMSO, 1 or 10 nM RA ± 1 μM dexamethasone (n = 6, ***p < 0.001 vs. 0.1% DMSO, ###p < 0.001 vs. RA).

(G) HepG2 cells were treated 6 h with 0.1% DMSO or 1 nM RA ± increasing concentrations of cortisol or dexamethasone (n = 3, *p < 0.05 **p < 0.01 vs. RA only group).

(H) HepG2 cells were treated 3 h with 100 nM RA (n = 3 replicates). The elimination t½ of RA was determined in the presence and absence of 100 nM dexamethasone, by quantifying ln % remaining in cells by LC/MS/MS. Both slopes differed significantly from 0, p < 0.02.

(I) Primary human hepatocytes were treated 6 h with 0.1% DMSO or 1 nM RA ± 100 nM dexamethasone (n = 4, ***p < 0.001 vs. 0.1% DMSO, ##p < 0.01 vs. RA).

See also SF1, SF2, SF3.

Dexamethasone-induced *CYP26A1* repression occurs at or near RA response elements

Dex did not increase the rate of *CYP26A1* mRNA degradation (Figure S3), consistent with arresting transcription. DR5 RARE has been mapped to the *CYP26A1* promoter (Loudig et al., 2000, 2005;

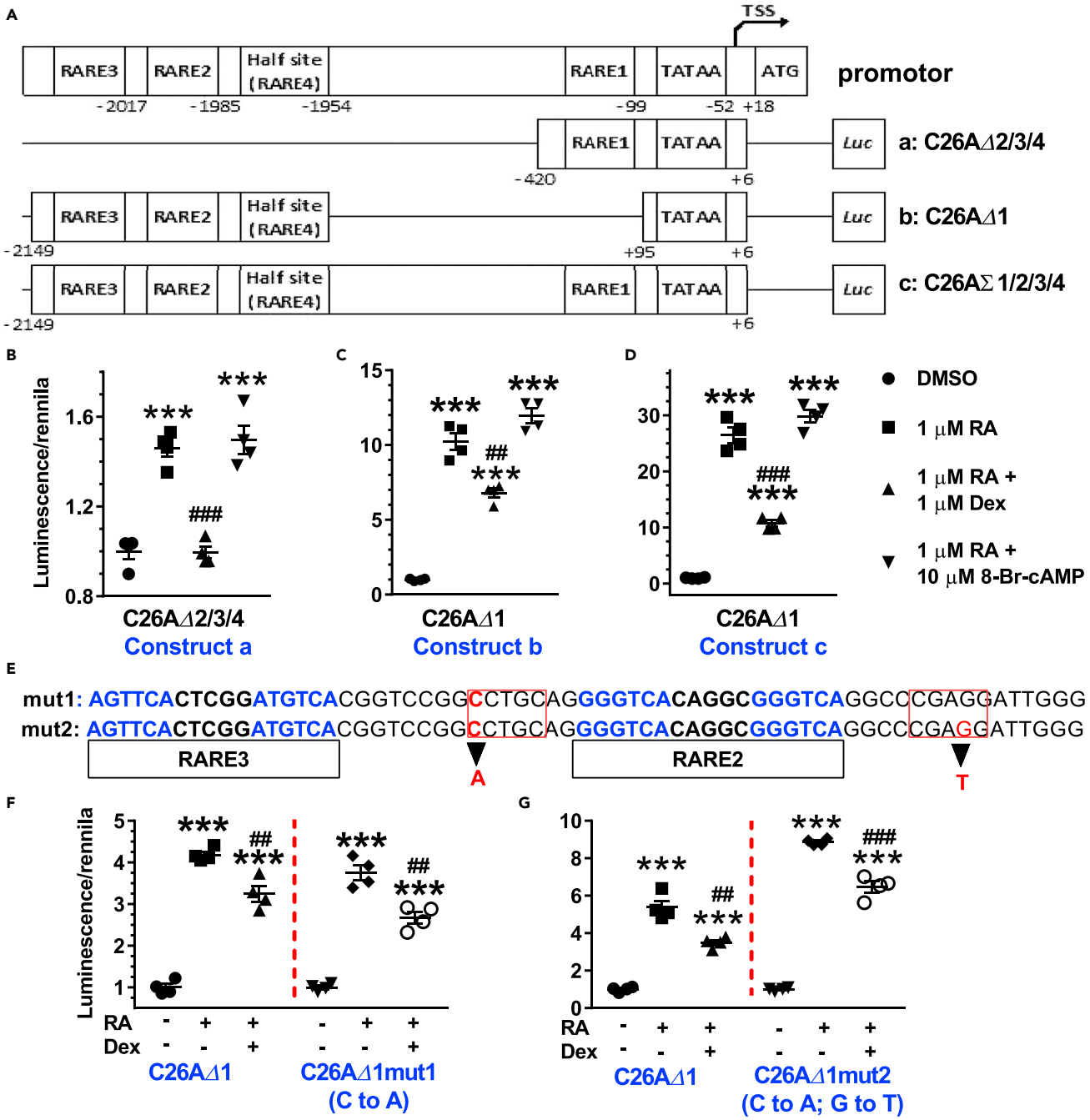

Figure 2. Dexamethasone-induced *CYP26A1* repression occurs at or near RAREs

(A) *CYP26A1* promoter and reporter vector constructs.

(B–D) HepG2 transfected with Luc reporter vector a (B), b (C), or c (D) were treated with 0.1% DMSO, 1 μM RA ± 1 μM dexamethasone or 10 μM 8-Br-cAMP (***p < 0.001 vs. DMSO; ##p < 0.01, ###p < 0.001 vs. 1 μM RA).

(E) Diagram of two variants of the C26AΔ1 construct generated by site-directed point mutagenesis. The red boxes indicate the putative GR binding sites.

(F) HepG2 transfected with C26AΔ1, C26AΔ1mut1 (C to A), or C26AΔ1mut2 (C to A and. G to T) were compared for Dex responsiveness (***p < 0.001 vs. 0.1% DMSO, ##p < 0.01, ###p < 0.001 vs. 1 μM RA). See also SF4, SF5, SF6.

Zhang et al., 2010). Based on the *cis*-acting RAREs that have been identified, we constructed three *Luc* reporter vectors, hypothesizing that these and/or adjacent sequences serve as sites of repression (Figure 2A).

Construct a, which includes only RARE1, responded to RA with ~50% increase of luminescence in HepG2 cells (Figure 2B). Dex nearly totally prevented RA induction of construct a. Construct b, which includes RARE2/3/4 but not RARE1, responded to RA with ~10-fold higher luminescence than DMSO Figure 2C). Dex suppressed RA induction of construct b by ~40%. Construct c, which replicates wild-type, responded to RA with ~26-fold increase in luminescence (Figure 2D). Dex inhibited RA induction of construct c by ~55%. These data indicate that RARE2/3/4 has the stronger effect on transcription. RARE1 alone has a lesser effect, but apparently synergizes with RARE2/3/4. Overall repression of construct c's expression seems a combination of each RARE's induction potency and the Dex effect. This suggests that Dex represses through a combination of both RARE1 and RARE2/3/4. Given these data and because the RAR/RXR heterodimer resides on RARE regardless of RA-binding, we excluded the hypothesis that the RAR/RXR heterodimer and the GR/GR homodimer compete for the same RARE (Iskakova et al., 2015). We hypothesized that GR binds to a locus adjacent to an RARE or to an RAR-RXR transcription-regulation complex. To the best of our knowledge, no ChIP-seq data have demonstrated GR binding up-stream (to ~5,000 bp) of *CYP26A1* in any human or mouse liver model. Therefore, we applied PROMO (ver. 3.0.2), a computational transcription factor search tool, to locate potential GR binding sites (Messeguer et al., 2002). Using site-directed mutagenesis, we introduced point mutations in two putative GR binding sites that flank but do not overlap RARE2 Figure 2E). Figure S4 describes the putative GR binding sites estimated by PROMO and loci of introduced mutations. Neither one point mutation (mut1: C to A) nor two point mutations (mut2: C to A and G to T) decreased responsiveness to Dex (Figure 2F).

Transient interaction between GR and an activated RAR/RXR complex represses *CYP26A1* expression

Negative results from site-directed mutagenesis could imply that the GR interacts with an RAR-RXR co-activation protein complex, rather than through a GR response element (GRE) interaction or GR binding on or near an RARE. We verified GR involvement using a GR antagonist, RU486. RU486 prevented the Dex effect on RA-induced *CYP26A1* expression (Figure S5). We then tested whether histone deacetylase (HDAC) mediates *CYP26A1* repression by the GR using the HDAC inhibitor trichostatin A (TSA). HDAC contributes to the RAR/RXR co-repressor complex that binds to DR5 RARE, which includes SIN3, N-CoR, and SMRT (Hörlein et al., 1995; Chen et al., 1996; Al Tanoury et al., 2013). Inhibition by TSA would indicate that the GR promotes formation of an RARE corepessor complex including recruitment of HDAC (Chen and Evans, 1995; Heinzel et al., 1997). TSA increased *CYP26A1* mRNA 2.5-fold in the presence of RA but had no effect on Dex repression of RA-induced *CYP26A1* mRNA (Figure S6). This suggests that the GR does not function through an HDAC-containing corepessor complex associated with RAR. Next, we designed a ChIP-qPCR experiment, scanning RARE1 and RARE2/3/4 upstream of *CYP26A1* and a GRE-RARE, upstream of the phosphoenolpyruvate carboxykinase 1 gene (*PCK1*), as a positive control. RARα was associated with the *PCK1* promoter in the presence and absence of RA, consistent with constitutive association of RAR with the *PCK1* RARE (Figure 3A). The same results occurred with Dex and the combination of Dex and RA, as expected for constitutive residence of RAR on the *PCK1* RARE. RARα was also associated with RARE2/3/4 of the *CYP26A1* promoter, regardless of treatment, also consistent with constitutive binding to the RARE. RARγ enrichment occurred at a much lower intensity, consistent with having a much lower presence in HepG2 cells (Tay et al., 2010; Li et al., 2013) (Figure 3B). GR enrichment in the *PCK1* promoter was not affected by RA, but Dex increased the GR association nearly by 2.5-fold. RA amplified the Dex effect further by 2.5-fold (Figure 3C). The Dex effect on GR enrichment in RARE1 and RARE2/3/4 requires RA, as neither RA alone nor Dex alone was effective. This indicates that the GR interaction occurs only with an RA-bound RAR-RXR coactivation complex. We next conducted a co-immunoprecipitation assay (Figure 3D). Western blot detected the GR following immunoprecipitation with a RARα antibody when cells were treated with disuccinimidyl glutarate (DSG), a protein cross-linker. Without DSG, there was no GR band. In addition, the GR was not detected when cells were treated with Dex for 1 h, even though its repressive effect lasts at least several hours (Figure S7).

C/EBPβ enhances *CYP26A1* expression: SNP rs2068888 regulates the C/EBPβ effect

A genome-wide association study (GWAS) has associated the minor allele (adenine) of SNP rs2068888 with a 2.28 mg/dL reduction in blood triglycerides. *CYP26A1* is the nearest annotated gene to the SNP (Teslovich et al., 2010). A major allele of rs2068888 has been linked to increased acute coronary syndrome risk in the AIM-HIGH (Atherothrombosis Intervention in Metabolic Syndrome with Low HDL/High Triglycerides and Impact on Global Health Outcomes) trial (Tuteja et al., 2018). ChIP-seq assays have revealed that the C/EBPβ binds to the SNP in five different human cell lines, including HepG2 (Partridge et al., 2020).

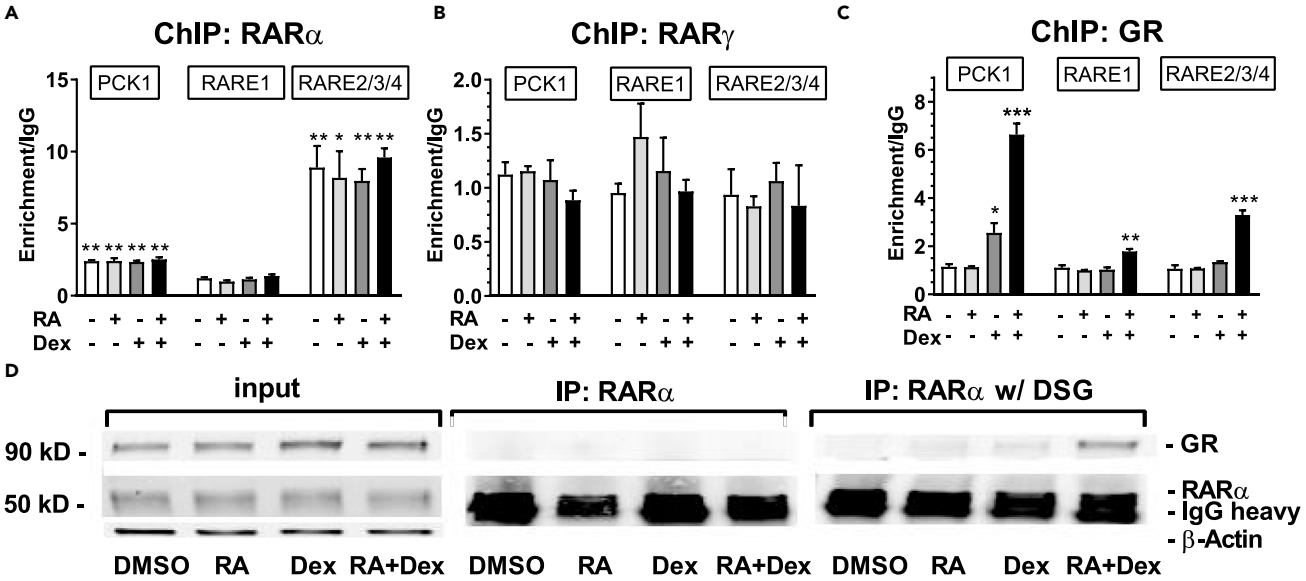

Figure 3. Transient interaction between GR and an activated RAR/RXR complex represses *CYP26A1* expression

(A–C) HepG2 cells were treated 30 min with 0.1% DMSO or 1 nM RA ± 100 nM Dex, followed by crosslinking, lysis, and sonication for ChIP. Chromatin samples were reacted with RARα (A), RARγ (B), or GR (C) antibodies. DNA samples obtained by reverse-crosslinking were used for qPCR with primers designed to scan (i) the GRE + RARE of the PCK1 promoter (positive control), (ii) RARE1, and (iii) RARE2/3/4 in the CYP26A1 promoter.

(D) Co-immunoprecipitation without over-expression. HepG2 were treated with 0.1% DMSO or 1 nM RA ± 100 nM Dex. A set of treatment groups was treated with crosslinker DSG. Isolated protein samples were immunoprecipitated with RARα antibody. The precipitated complex was resolved by western blotting using a GR antibody. See also SF7, SF8.

RegulomeDB evaluates the SNP as "likely to affect binding" to C/EBPβ (Boyle et al., 2012). Based on these data, we hypothesized that 1) C/EBPβ binding to the major allele of the SNP enhances *CYP26A1* expression and 2) the minor allele reduces C/EBPβ binding to the SNP, thereby decreasing *CYP26A1* expression. RA does not induce *CEBPB* transcription, indicated by no increase with time after exposure to RA (Figure 4A). A siRNA knockdown of *CEBPB* reduced its expression by 50% in HepG2 cells, which decreased RA-induced *CYP26A1* expression by 46 to 67% (Figure 4B). This result complements the C/EBPβ inhibitor genistein, which repressed *CYP26A1* expression in HepG2/C3A cells (Harmon et al., 2002; Lepri et al., 2018). We confirmed the ability of genistein to repress RA-induced *CYP26A1* expression in HepG2 cells (Figure S8). We conducted ChIP-qPCR to test effects of RA and Dex on C/EBPβ induction of *CYP26A1*. RA recruited C/EBPβ to the vicinity of the SNP (Figure 4C). Dex did not interfere with the RA effect. Dex, however, promoted association of RA-liganded RARα with the SNP. Dex treatment also enriched C/EBPβ in RARE1 of the *CYP26A1* promoter (Figure 4D). C/EBPβ association with RARE2/3/4 was not affected by RA, Dex, or the combination. We then generated an rs2068888 model system in HeLa cells, which are more amenable to CRISPR/Cas9 mutation than HepG2 cells. A single-base edit, G to A, increased the minor allele frequency from ~33 to 50% (Figure 4E). C/EBPβ enrichment increased ~3-fold in WT HeLa cells treated with RA, which Dex did not affect (Figure 4F). Dex decreased RA induction of *CYP26A1* mRNA in WT HeLa cells ~50% (Figure 4G). In contrast, edited cells did not respond to RA or Dex (Figure 4G).

DISCUSSION

The current data show that 1) Dex and glucagon reduce RA-induction of *CYP26A1* (Figures 1B, 1C, and 1E, Figures 2B–2D); 2) Dex does not alter constitutive binding of RARα to RARE (Figure 3A); and 3) the GR binds to an RAR/RXR co-transcription complex only in the presence of RA (Figures 3A, 3C, 3D, and S3B). These data indicate that Dex weakens RA induction of *CYP26A1* by promoting an inhibitory GR interaction with an RAR/RXR coactivation complex associated with a RARE. The GR thereby impairs RA induction of *CYP26A1* expression during the fasted state to preserve a higher RA concentration than during feeding.

Insulin, via expelling FoxO1 from the nucleus, reduces *Rdh1* and *Rdh10* transcription, resulting in a 50% decrease in the RA liver concentration relative to fasting (Obrochta et al., 2015). Data here complement the insight that RA levels are highest during fasting, by revealing that hormones secreted during fasting

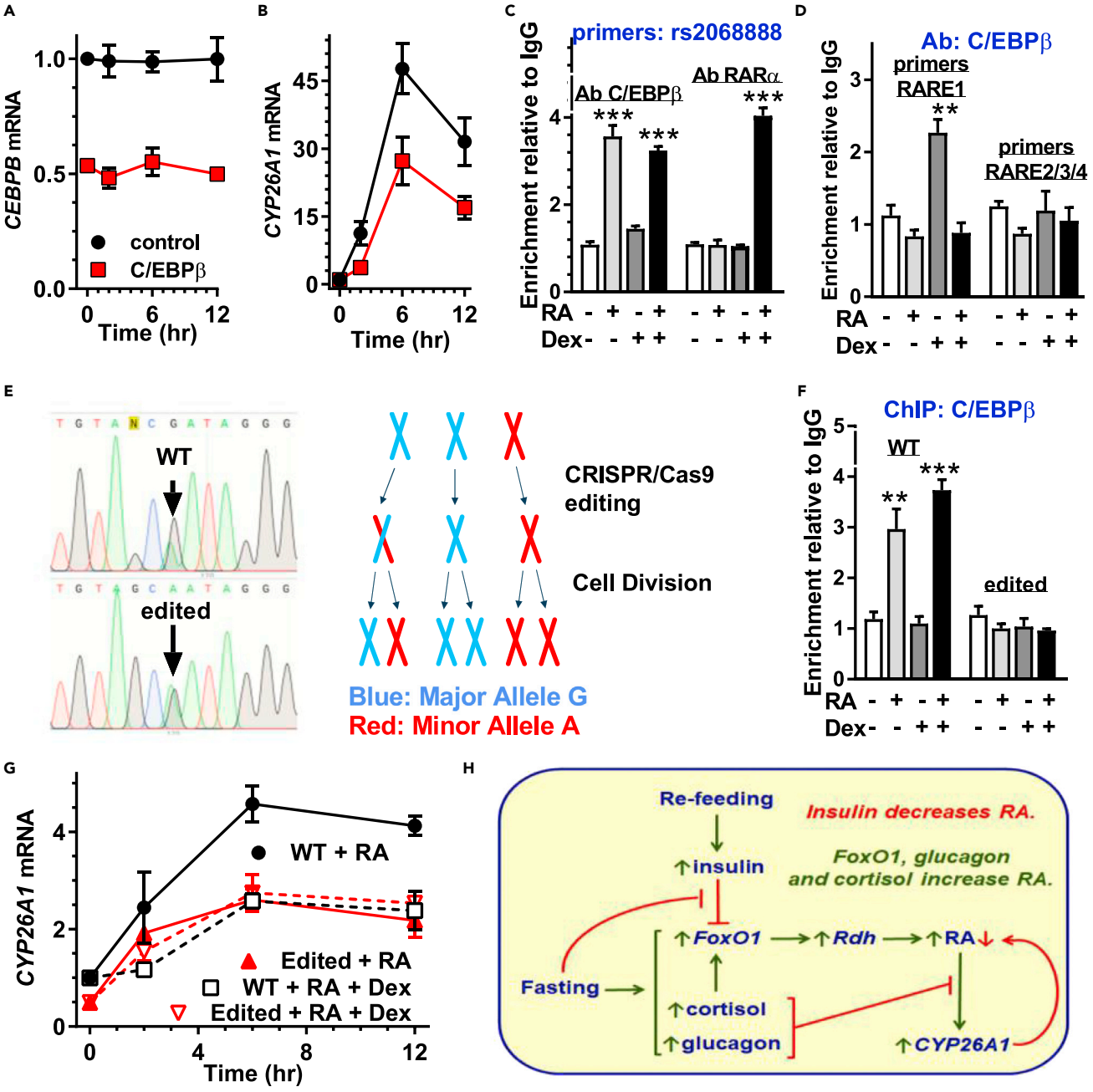

Figure 4. C/EBPβ enhances *CYP26A1* expression: SNP rs2068888 retards C/EBPβ modulation of *CYP26A1*

(A and B) HepG2 cells cultured in EMEM containing 10% charcoal-stripped FBS were transfected 24 h with scrambled siRNA (control) or siRNA, then treated with 1 nM RA in FBS-free medium (n = 3). WT differed significantly from siRNA in both A and B: $p < 0.001$, two-way ANOVA. (A) Time-course of *CEBPB* mRNA (controls, black circles; siRNA, red squares). (B) Time-course of *CYP26A1 mRNA* in the presence of siRNA controls and siRNA CEBPB (controls, black circles; siRNA, red squares) (n = 3).

(C and D) HepG2 cells were treated 30 min with 0.1% DMSO or 1 nM RA ± 100 nM Dex, followed by crosslinking, lysis, and sonication for ChIP. DNA samples obtained by reversing crosslinking were used in qPCR with primers designed to amplify RARE1 and RARE2/3/4 in the *CYP26A1* promoter or C/EBPβ and RARα in SNP rs2068888. Antibodies were applied against C/EBPβ or RARα.

(E) Chromatogram showing DNA sequencing of WT HeLa vs. CRISPR-edited cells. HeLa cells have trisomy in chromosome 10: two with the major allele and another with the minor allele, deriving ~33% minor allele frequency. CRISPR editing introduced one copy of a single base replacement (G to A), resulting in a 50% minor allele frequency after a cycle of cell division.

(F) Effects of RA and Dex on C/EBPβ enrichment of rs2068888 in WT and edited HeLa cells.

Figure 4. *Continued*

(G) Time-course of 1 nM RA ± Dex effects on *CYP26A1* mRNA in WT and CRISPR-edited HeLa cells (n = 3, $p \leq 0.0001$ by two-way ANOVA for Dex and gene edited effects). (H) Regulation of RA homeostasis by fasting and refeeding. During fasting FoxO1 activity induces *Rdh* transcriptionally. RA induces *CYP26A1*. To prevent futile cycling during fasting, glucagon and cortisol retard *CYP26A1* transcription. During refeeding, insulin causes FoxO1 to leave the nucleus and undergo proteolysis. This decreases Rdh and RA. Inhibition of *CYP26A1* expression ceases allowing RA to auto-induce its catabolism. These actions result in higher RA during fasting vs refeeding, permitting RA to antagonize insulin action during fasting, while permitting optimum insulin action during feeding.

suppress RA catabolism by reducing *CYP26A1* mRNA and activity. RA serves as a potent inducer of *CYP26A1* transcription (White et al., 1996; Ray et al., 1997, and current data). This presents a potential contradiction. Increasing RA during fasting should enhance *CYP26A1* transcription to reduce RA levels, rendering short-lived substantial RA increase. The demonstration that hormones secreted during fasting impair *CYP26A1* transcription and activity indicates a mechanism for maintaining increased RA concentrations during fasting. Thus, control of CYP26A1 seems essential to RA regulating energy balance in the transition between fasting and re-feeding. Figure 4H presents a model of regulation during changes in energy status, illustrating the contributions of insulin, glucagon, and cortisol to RA biosynthesis vs catabolism.

Cyp26a1 mRNA decreases in the livers of mice injected with Dex (Surjit et al., 2011). A mechanism suggested was recruitment of a GR-SMRT/NCoR repressing complex onto a negative GRE located on an intron of neighboring gene *Cyp26c1*, 8,287 (mouse), or 8,851 bp (human) upstream of *Cyp26a1*/*CYP26A1*. The current data show an alternative and/or coexisting mechanism. Another study showed that oral treatment with lipopolysaccharide (LPS) or poly-I:C suppresses RA-induced *Cyp26a1* expression in rat liver (Zolfaghari et al., 2007). The present data complement this observation because LPS stimulates cortisol secretion (Vakharia and Hinson, 2005). A liver-specific mouse GR knockout resulted in a 2.3-fold increase in *Cyp26a1* expression, which supports GR-mediated *Cyp26a1* repression (Engblom et al., 2007). Contrary to these findings, an increase in hepatic *Cyp26a1* mRNA mediated by the pregnane X receptor was reported in mice treated with Dex (Wang et al., 2008). This study relied on chronically dosing toxic RA concentrations *in vivo* (10 mg/kg) and used *in vitro* concentrations ~1000-fold higher (5 μM) than physiological because it evaluated RA as an anti-cancer treatment. Under these conditions, the report concluded that CYP26A1 does not serve as the major RA catabolic enzyme in the liver. The hormesis effects of RA likely affected this outcome, relative to physiological concentrations (Napoli, 2020).

Several mechanisms by which the GR suppresses transcription have been suggested: GR-(n)GRE binding, disruption of transcriptional elongation, chromatin remodeling, and tethering to transcription factors (Granner et al., 2015). Our data propose a role of nuclear co-activators in recruiting GR because GR enrichment did not increase in the absence of RA, indicating that GR doesn't bind to an RAR/RXR corepessor complex. In a RARα-RXRα-DR5 model, a primary co-activator of the p160 family (SRC1 or TIF2) binds to LxxLL binding motifs of both RARα and RXRα, which associates the RAR-RXR activation complex with pol II transcription machinery (Osz et al., 2012; Rochel et al., 2011; Senicourt et al., 2021). In fact, the TIF2 co-activator reportedly interacts with the GR to activate or suppress gene expression. For instance, TIF2/GRIP1 is recruited to AP-1 subunits to facilitate GR-mediated repression of the collagenase-3 gene (Rogatsky et al., 2001). Thus, TIF2/GRIP1, a part of the RAR-RXR activation complex, could function as a switch to suppress *CYP26A1* expression by interaction with the GR.

The present data further show that 4) RA does not increase C/EBPβ transcription in HepG2 cells (Figure 4A); 5) C/EBPβ enhances *Cyp26A1* transcription (a *CEBPB* knockdown decreases *CYP26A1* transcription) (Figures 4A and 4B); 6) RA increases C/EBPβ association with SNP rs2068888; this is not blocked by Dex (Figure 4C); 7) Dex increases C/EBPβ association with a transcriptional complex associated with RARE1 in the absence of RA, suggesting a corepressor interaction (Figure 4D); 8) RA and Dex together increase RARα binding to SNP rs2068888, but neither alone has an effect (Figure 4C); 9) the minor allele prevents C/EBPβ binding to the SNP (Figure 4F); 10) the minor allele of the SNP inhibits RA induction of *CYP26A1* (Figure 4G). These data indicate specific actions of RA vs Dex concerning C/EBPβ induction of *CYP26A1*. Namely, RA recruits C/EBPβ to the major allele of SNP rs206888, which enhances *CYP26A1* transcription, an effect diminished by the minor allele. By decreasing RA-induced *CYP26A1* transcription, the minor allele promotes an increase in liver RA. These data suggest another mechanism of GR action; reducing C/EBPβ-enhanced *CYP26A1* transcription. Plausibly, this would occur by Dex promoting C/EBPβ association with a ligand unoccupied RAR bound to RARE1, i.e., a corepressor complex. Recruitment of RARα to the SNP by Dex in the presence of RA suggests another potential mechanism whereby the GR would inhibit RA-induced *CYP26A1* transcription.

C/EBPβ interacts with other transcription regulators, including the GR, nuclear factor Kappa B, and Activator Protein-1, to increase chromatin opening (Davis et al., 2018; Grøntved et al., 2013; Kabotyanski

et al., 2006; Lane et al., 1999). C/EBPβ binding sites have been mapped to promoters regulated by retinoids (Elizondo et al., 2000; Wang et al., 2001), and an interaction between C/EBPβ and the RAR/RXR transcription complex occurs during adipogenesis (Schwarz et al., 1997). These data suggest that C/EBPβ augments RA-induced *CYP26A1* transcription by contributing to chromatin opening. The ability of C/EBPβ to interact with both rs2068888 and RARE1 indicates that C/EBPβ/rs2068888 likely locates to the vicinity of RARE1 in 3D genomic space, and/or C/EBPβ may transfer between rs2068888 and RARE1 in the *CYP26A1* promoter region depending on metabolic status. SMRT (Silencing Mediator of Retinoid and Thyroid Hormone Receptors), an element of the RAR/RXR corepessor complex, binds to the transactivation domain of C/EBPβ, which represses *GSTA2* expression (Ki et al., 2005). Thus, it is reasonable to suggest that C/EBPβ transfers from rs2068888 to the RAR repression complex associated with SMRT or a 3-dimensional association of C/EBPβ bound to rs2068888, and SMRT closes chromatin in the *CYP26A1* promoter region, contributing to epigenetic prevention of transcription.

GWASs have mapped thousands of loci to complex traits (Gallagher and Chen-Plotkin, 2018).

These associations may reveal underlying mechanisms disrupted in various diseases. It is difficult, however, to verify which genes these loci regulate and in which tissues or circumstances regulation develops. Hence, GWAS findings are translated slowly into drug development or clinical therapy. Although *CYP26A1* is the nearest gene from SNP rs2068888, there has been no human expression quantitative trait loci data associating the SNP alleles with CYP26A1. We demonstrated an rs2068888-allele-dependent change in *CYP26A1* expression, which explains the lower level of blood triglyceride in the population with the minor allele, as the increase in RA would diminish VLDL (very low density lipoprotein) particle secretion from liver (Amengual et al., 2010; Li et al., 2013).

The current data provide new insight into retinoid regulation of energy metabolism, glucoregulatory control, mechanisms of the GR regulating RAR-driven gene expression, and Cyp26a1 effects on retinoid functions.

Limitations of the study

Much remains to learn about the mechanism(s) of the GR interaction with RAR and C/EBPβ. This report established interactions but focused on the physiological significance of regulating *CYP26A1* transcription during fasting to prevent counter-productive RA oxidation. We showed that RA in the whole liver varies with fasting and refeeding and explored mechanisms in hepatocytes, which provide 90% of liver cells. Yet, contributions of other liver cell types cannot be excluded.

STAR★METHODS

Detailed methods are provided in the online version of this paper and include the following:

- KEY RESOURCES TABLE
- RESOURCE AVAILABILITY
  - Lead contact
  - Materials availability
  - Data and code availability
- EXPERIMENTAL MODEL AND SUBJECT DETAILS
  - Animal experiments
  - Cell culture
- METHOD DETAILS
  - Gene expression assays
  - Quantification of RA in tissues and cells
  - Cloning reporter vectors
  - Transfection and luciferase assay
  - ChIP-qPCR
  - Co-immunoprecipitation and western blotting
  - Site-directed mutagenesis
  - CEBPB knock down
  - CRISPR/Cas9-mediated single 'base edit
  - DNA sequencing
- QUANTIFICATION AND STATISTICAL ANALYSIS

SUPPLEMENTAL INFORMATION

Supplemental information can be found online at https://doi.org/10.1016/j.isci.2022.104564.

ACKNOWLEDGMENTS

We thank Yaron Rotman at NIDDK for introducing LDlink (https://ldlink.nci.nih.gov/) and RegulomeDB (https://regulomedb.org/) and for helpful discussions and Karen Lundy at the UC Berkeley Functional Genomics Laboratory for chromatin shearing service. JLN was funded by NIH grants DK112754 and DK107773. SK was funded by NIH grant R01 DK116008.

AUTHOR CONTRIBUTIONS

H.S.Y. designed and conducted experiments, analyzed data, and wrote the manuscript. A.R. designed and performed experiments. D.Y. and R.A.L. helped design experiments and suggested experimental design. M.A.C. and J.A.G. conducted experiments and analyzed data. J-C.W. and S.K. provided expert input and contributed to experimental design. J.L.N. obtained funding, contributed to experimental design, analyzed data, and edited the manuscript.

DECLARATION OF INTERESTS

The authors declare no competing interests.

Received: November 19, 2021
Revised: May 12, 2022
Accepted: June 6, 2022
Published: July 15, 2022

REFERENCES

Abu-Abed, S.S., Beckett, B.R., Chiba, H., Chithalen, J.V., Jones, G., Metzger, D., Chambon, P., and Petkovich, M. (1998). Mouse P450RAI (CYP26) expression and retinoic acid-inducible retinoic acid metabolism in F9 cells are regulated by retinoic acid receptor gamma and retinoid X receptor alpha. J. Biol. Chem. *273*, 2409–2415. https://doi.org/10.1074/jbc.273.4.2409.

Abu-Abed, S., Dollé, P., Metzger, D., Beckett, B., Chambon, P., and Petkovich, M. (2001). The retinoic acid- metabolizing enzyme, CYP26A1, is essential for normal hindbrain patterning, vertebral identity, and development of posterior structures. Genes Dev. *15*, 226–240. https://doi.org/10.1101/gad.855001.

Al Tanoury, Z., Piskunov, A., and Rochette-Egly, C. (2013). Vitamin A and retinoid signaling: genomic and nongenomic effects. J. Lipid Res. *54*, 1761–1775. https://doi.org/10.1194/jlr.R030833.

Amengual, J., Ribot, J., Bonet, M.L., and Palou, A. (2010). Retinoic acid treatment enhances lipid oxidation and inhibits lipid biosynthesis capacities in the liver of mice. Cell. Physiol. Biochem. *25*, 657–666. https://doi.org/10.1159/000315085.

Arnold, S.L.M., Amory, J.K., Walsh, T.J., and Isoherranen, N. (2012). A sensitive and specific method for measurement of multiple retinoids in human serum with UHPLC-MS/MS. J. Lipid Res. *53*, 587–598. https://doi.org/10.1194/jlr.D019745.

Belyaeva, O.V., Adams, M.K., Popov, K.M., and Kedishvili, N.Y. (2019). Generation of retinaldehyde for retinoic acid biosynthesis. Biomolecules *10*. https://doi.org/10.3390/biom10010005.

Berry, D.C., DeSantis, D., Soltanian, H., Croniger, C.M., and Noy, N. (2012). Retinoic acid upregulates preadipocyte genes to block adipogenesis and suppress diet-induced obesity. Diabetes *61*, 1112–1121. https://doi.org/10.2337/db11-1620.

Berry, D.C., and Noy, N. (2009). All-trans-retinoic acid represses obesity and insulin resistance by activating both peroxisome proliferation-activated receptor beta/delta and retinoic acid receptor. Mol. Cell Biol. *29*, 3286–3296. https://doi.org/10.1128/MCB.01742-08.

Billings, S.E., Pierzchalski, K., Butler Tjaden, N.E., Pang, X.-Y., Trainor, P.A., Kane, M.A., and Moise, A.R. (2013). The retinaldehyde reductase DHRS3 is essential for preventing the formation of excess retinoic acid during embryonic development. FASEB J. *27*, 4877–4889. https://doi.org/10.1096/fj.13-227967.

Boyle, A.P., Hong, E.L., Hariharan, M., Cheng, Y., Schaub, M.A., Kasowski, M., Karczewski, K.J., Park, J., Hitz, B.C., Weng, S., et al. (2012). Annotation of functional variation in personal genomes using RegulomeDB. Genome Res. *22*, 1790–1797. https://doi.org/10.1101/gr.137323.112.

Chen, J.D., and Evans, R.M. (1995). A transcriptional co-repressor that interacts with nuclear hormone receptors. Nature *377*, 454–457. https://doi.org/10.1038/377454a0.

Chen, J.D., Umesono, K., and Evans, R.M. (1996). SMRT isoforms mediate repression and anti-repression of nuclear receptor heterodimers. Proc. Natl. Acad. Sci. USA *93*, 7567–7571. https://doi.org/10.1073/pnas.93.15.7567.

Cione, E., Caroleo, M.C., Cannataro, R., Perri, M., Pingitore, A., and Genchi, G. (2016). Vitamin A and diabesity: new insight for drug discovery. Mini Rev. Med. Chem. *16*, 738–742. https://doi.org/10.2174/1389557515666150709112822.

Das, B.C., Thapa, P., Karki, R., Das, S., Mahapatra, S., Liu, T.-C., Torregroza, I., Wallace, D.P., Kambhampati, S., Van Veldhuizen, P., et al. (2014). Retinoic acid signaling pathways in development and diseases. Bioorg. Med. Chem. *22*, 673–683. https://doi.org/10.1016/j.bmc.2013.11.025.

Davis, C.A., Hitz, B.C., Sloan, C.A., Chan, E.T., Davidson, J.M., Gabdank, I., Hilton, J.A., Jain, K., Baymuradov, U.K., Narayanan, A.K., et al. (2018). The Encyclopedia of DNA elements (ENCODE): data portal update. Nucleic Acids Res. *46*, D794–D801. https://doi.org/10.1093/nar/gkx1081.

E, X., Zhang, L., Lu, J., Tso, P., Blaner, W.S., Levin, M.S., and Li, E. (2002). Increased neonatal mortality in mice lacking cellular retinol-binding protein II. J. Biol. Chem. *277*, 36617–36623. https://doi.org/10.1074/jbc.M205519200.

Elizondo, G., Corchero, J., Sterneck, E., and Gonzalez, F.J. (2000). Feedback inhibition of the retinaldehyde dehydrogenase gene ALDH1 by retinoic acid through retinoic acid receptor alpha and CCAAT/enhancer- binding protein beta. J. Biol. Chem. *275*, 39747–39753. https://doi.org/10.1074/jbc.M004987200.

Engblom, D., Kornfeld, J.-W., Schwake, L., Tronche, F., Reimann, A., Beug, H., Hennighausen, L., Moriggl, R., and Schütz, G. (2007). Direct glucocorticoid receptor–Stat5 interaction in hepatocytes controls body size and maturation-related gene expression. Genes Dev.

21, 1157–1162. https://doi.org/10.1101/gad.426007.

Gallagher, M.D., and Chen-Plotkin, A.S. (2018). The post-GWAS era: from association to function. Am. J. Hum. Genet. *102*, 717–730. https://doi.org/10.1016/j.ajhg.2018.04.002.

Gewiss, R., Topping, T., and Griswold, M.D. (2020). Cycles, waves, and pulses: retinoic acid and the organization of spermatogenesis. Andrology *8*, 892–897. https://doi.org/10.1111/andr.12722.

Granner, D.K., Wang, J.-C., and Yamamoto, K.R. (2015). Regulatory actions of glucocorticoid hormones: from organisms to mechanisms. Adv. Exp. Med. Biol. *872*, 3–31. https://doi.org/10.1007/978-1-4939-2895-8_1.

Grøntved, L., John, S., Baek, S., Liu, Y., Buckley, J.R., Vinson, C., Aguilera, G., and Hager, G.L. (2013). C/EBP maintains chromatin accessibility in liver and facilitates glucocorticoid receptor recruitment to steroid response elements. EMBO J. *32*, 1568–1583. https://doi.org/10.1038/emboj.2013.106.

Harmon, A.W., Patel, Y.M., and Harp, J.B. (2002). Genistein inhibits CCAAT/enhancer-binding protein beta (C/EBPbeta) activity and 3T3-L1 adipogenesis by increasing C/EBP homologous protein expression. Biochem. J. *367*, 203–208. https://doi.org/10.1042/BJ20020300.

Heinzel, T., Lavinsky, R.M., Mullen, T.-M., Söderström, M., Laherty, C.D., Torchia, J., Yang, W.-M., Brard, G., Ngo, S.D., Davie, J.R., et al. (1997). A complex containing N-CoR, mSin3 and histone deacetylase mediates transcriptional repression. Nature *387*, 43–48. https://doi.org/10.1038/387043a0.

Hörlein, A.J., Näär, A.M., Heinzel, T., Torchia, J., Gloss, B., Kurokawa, R., Ryan, A., Kamei, Y., Söderström, M., and Glass, C.K. (1995). Ligand-independent repression by the thyroid hormone receptor mediated by a nuclear receptor co-repressor. Nature *377*, 397–404. https://doi.org/10.1038/377397a0.

Iskakova, M., Karbyshev, M., Piskunov, A., and Rochette-Egly, C. (2015). Nuclear and extranuclear effects of vitamin A. Can. J. Physiol. Pharmacol. *93*, 1065–1075. https://doi.org/10.1139/cjpp-2014-0522.

Isoherranen, N., and Zhong, G. (2019). Biochemical and physiological importance of the CYP26 retinoic acid hydroxylases. Pharmacol. Ther. *204*, 107400. https://doi.org/10.1016/j.pharmthera.2019.107400.

Kabotyanski, E.B., Huetter, M., Xian, W., Rijnkels, M., and Rosen, J.M. (2006). Integration of prolactin and glucocorticoid signaling at the beta-casein promoter and enhancer by ordered recruitment of specific transcription factors and chromatin modifiers. Mol. Endocrinol. *20*, 2355–2368. https://doi.org/10.1210/me.2006-0160.

Kane, M.A., Folias, A.E., Pingitore, A., Perri, M., Krois, C.R., Ryu, J.Y., Cione, E., and Napoli, J.L. (2011). Crbpl modulates glucose homeostasis and pancreas 9-cis-retinoic acid concentrations. Mol. Cell Biol. *31*, 3277–3285. https://doi.org/10.1128/MCB.05516-11.

Kane, M.A., Folias, A.E., Pingitore, A., Perri, M., Obrochta, K.M., Krois, C.R., Cione, E., Ryu, J.Y., and Napoli, J.L. (2010). Identification of 9-cis-retinoic acid as a pancreas-specific autacoid that attenuates glucose-stimulated insulin secretion. Proc. Natl. Acad. Sci. USA *107*, 21884–21889. https://doi.org/10.1073/pnas.1008859107.

Kane, M.A., Folias, A.E., Wang, C., and Napoli, J.L. (2008). Quantitative profiling of endogenous retinoic acid in vivo and in vitro by tandem mass spectrometry. Anal. Chem. *80*, 1702–1708. https://doi.org/10.1021/ac702030f.

Ki, S.H., Cho, I.J., Choi, D.W., and Kim, S.G. (2005). Glucocorticoid receptor (GR)-Associated SMRT binding to C/EBPβ TAD and Nrf2 Neh4/5: role of SMRT recruited to GR in GSTA2 gene repression. Mol. Cell Biol. *25*, 4150–4165. https://doi.org/10.1128/MCB.25.10.4150-4165.2005.

Kinkel, M.D., Sefton, E.M., Kikuchi, Y., Mizoguchi, T., Ward, A.B., and Prince, V.E. (2009). Cyp26 enzymes function in endoderm to regulate pancreatic field size. Proc. Natl. Acad. Sci. USA *106*, 7864–7869. https://doi.org/10.1073/pnas.0813108106.

Krois, C.R., Vuckovic, M.G., Huang, P., Zaversnik, C., Liu, C.S., Gibson, C.E., Wheeler, M.R., Obrochta, K.M., Min, J.H., Herber, C.B., et al. (2019). RDH1 suppresses adiposity by promoting brown adipose adaptation to fasting and re-feeding. Cell. Mol. Life Sci. *76*, 2425–2447. https://doi.org/10.1007/s00018-019-03046-z.

Lane, M.D., Tang, Q.-Q., and Jiang, M.-S. (1999). Role of the CCAAT enhancer binding proteins (C/EBPs) in adipocyte differentiation. Biochem. Biophys. Res. Commun. *266*, 677–683. https://doi.org/10.1006/bbrc.1999.1885.

Lepri, S.R., Sartori, D., Semprebon, S.C., Baranoski, A., Coatti, G.C., and Mantovani, M.S. (2018). Genistein affects expression of cytochrome P450 (CYP450) genes in hepatocellular carcinoma (HEPG2/C3A) cell line. Drug Metab. Lett. *12*, 138–144. https://doi.org/10.2174/1872312812666180709150440.

Li, Y., Wong, K., Walsh, K., Gao, B., and Zang, M. (2013). Retinoic acid receptor β stimulates hepatic induction of fibroblast growth factor 21 to promote fatty acid oxidation and control whole-body energy homeostasis in mice. J. Biol. Chem. *288*, 10490–10504. https://doi.org/10.1074/jbc.M112.429852.

Lin, Y.-W., Park, S.W., Lin, Y.-L., Burton, F.H., and Wei, L.-N. (2020). Cellular retinoic acid binding protein 1 protects mice from high-fat diet-induced obesity by decreasing adipocyte hypertrophy. Int. J. Obes. *44*, 466–474. https://doi.org/10.1038/s41366-019-0379-z.

Liu, L., and Gudas, L.J. (2005). Disruption of the lecithin:retinol acyltransferase gene makes mice more susceptible to vitamin A deficiency. J. Biol. Chem. *280*, 40226–40234. https://doi.org/10.1074/jbc.M509643200.

Lorberbaum, D.S., Kishore, S., Rosselot, C., Sarbaugh, D., Brooks, E.P., Aragon, E., Xuan, S., Simon, O., Ghosh, D., Mendelsohn, C., et al. (2020). Retinoic acid signaling within pancreatic endocrine progenitors regulates mouse and human β cell specification. Development *147*, dev189977. https://doi.org/10.1242/dev.189977.

Loudig, O., Babichuk, C., White, J., Abu-Abed, S., Mueller, C., and Petkovich, M. (2000). Cytochrome P450RAI(CYP26) promoter: a distinct composite retinoic acid response element underlies the complex regulation of retinoic acid metabolism. Mol. Endocrinol. *14*, 1483–1497. https://doi.org/10.1210/mend.14.9.0518.

Loudig, O., Maclean, G.A., Dore, N.L., Luu, L., and Petkovich, M. (2005). Transcriptional co-operativity between distant retinoic acid response elements in regulation of Cyp26A1 inducibility. Biochem. J. *392*, 241–248. https://doi.org/10.1042/BJ20050874.

Martín, M., Gallego-Llamas, J., Ribes, V., Kedinger, M., Niederreither, K., Chambon, P., Dollé, P., and Gradwohl, G. (2005). Dorsal pancreas agenesis in retinoic acid-deficient Raldh2 mutant mice. Dev. Biol. *284*, 399–411. https://doi.org/10.1016/j.ydbio.2005.05.035.

Messeguer, X., Escudero, R., Farré, D., Núñez, O., Martínez, J., and Albà, M.M. (2002). PROMO: detection of known transcription regulatory elements using species-tailored searches. Bioinformatics *18*, 333–334. https://doi.org/10.1093/bioinformatics/18.2.333.

Miyazaki, S., Taniguchi, H., Moritoh, Y., Tashiro, F., Yamamoto, T., Yamato, E., Ikegami, H., Ozato, K., and Miyazaki, J. (2010). Nuclear hormone retinoid X receptor (RXR) negatively regulates the glucose- stimulated insulin secretion of pancreatic ß-cells. Diabetes *59*, 2854–2861. https://doi.org/10.2337/db09-1897.

Napoli, J.L. (2020). Post-natal all-trans-retinoic acid biosynthesis. Methods Enzymol. *637*, 27–54. https://doi.org/10.1016/bs.mie.2020.02.003.

Napoli, J.L. (2012). Physiological insights into all-trans-retinoic acid biosynthesis. Biochim. Biophys. Acta *1821*, 152–167. https://doi.org/10.1016/j.bbalip.2011.05.004.

Napoli, J.L. (2022). Retinoic acid: sexually dimorphic, anti-insulin and concentration-dependent effects on energy. Nutrients *14*, 1553. https://doi.org/10.3390/nu14081553.

Noy, N. (2013). The one-two punch: retinoic acid suppresses obesity both by promoting energy expenditure and by inhibiting adipogenesis. Adipocyte *2*, 184–187. https://doi.org/10.4161/adip.23489.

Obrochta, K.M., Kane, M.A., and Napoli, J.L. (2014). Effects of diet and strain on mouse serum and tissue retinoid concentrations. PLoS One *9*, e99435. https://doi.org/10.1371/journal.pone.0099435.

Obrochta, K.M., Krois, C.R., Campos, B., and Napoli, J.L. (2015). Insulin regulates retinol dehydrogenase expression and all-trans-retinoic acid biosynthesis through FoxO1. J. Biol. Chem. *290*, 7259–7268. https://doi.org/10.1074/jbc.M114.609313.

Osz, J., Brélivet, Y., Peluso-Iltis, C., Cura, V., Eiler, S., Ruff, M., Bourguet, W., Rochel, N., and Moras, D. (2012). Structural basis for a molecular allosteric control mechanism of cofactor binding to nuclear receptors. Proc. Natl. Acad. Sci. USA *109*, E588–E594. https://doi.org/10.1073/pnas.1118192109.

Partridge, E.C., Chhetri, S.B., Prokop, J.W., Ramaker, R.C., Jansen, C.S., Goh, S.-T., Mackiewicz, M., Newberry, K.M., Brandsmeier, L.A., Meadows, S.K., et al. (2020). Occupancy

maps of 208 chromatin-associated proteins in one human cell type. Nature *583*, 720–728. https://doi.org/10.1038/s41586-020-2023-4.

Pennimpede, T., Cameron, D.A., MacLean, G.A., Li, H., Abu-Abed, S., and Petkovich, M. (2010). The role of CYP26 enzymes in defining appropriate retinoic acid exposure during embryogenesis. Birth Defects Res. A Clin. Mol. Teratol. *88*, 883–894. https://doi.org/10.1002/bdra.20709.

Pino-Lagos, K., Guo, Y., and Noelle, R.J. (2010). Retinoic acid: a key player in immunity. Biofactors *36*, 430. https://doi.org/10.1002/biof.117.

Pratt, W.B., Kaine, J.L., and Pratt, D.V. (1975). The kinetics of glucocorticoid binding to the soluble specific binding protein of mouse fibroblasts. J. Biol. Chem. *250*, 4584–4591.

Quadro, L., Blaner, W.S., Salchow, D.J., Vogel, S., Piantedosi, R., Gouras, P., Freeman, S., Cosma, M.P., Colantuoni, V., and Gottesman, M.E. (1999). Impaired retinal function and vitamin A availability in mice lacking retinol-binding protein. EMBO J. *18*, 4633–4644. https://doi.org/10.1093/emboj/18.17.4633.

Ray, W.J., Bain, G., Yao, M., and Gottlieb, D.I. (1997). CYP26, a novel mammalian cytochrome P450, is induced by retinoic acid and defines a new family. J. Biol. Chem. *272*, 18702–18708. https://doi.org/10.1074/jbc.272.30.18702.

Reeves, P.G. (1997). Components of the AIN-93 diets as improvements in the AIN-76A diet. J. Nutr. *127*, 838S–841S. https://doi.org/10.1093/jn/127.5.838S.

Rochel, N., Ciesielski, F., Godet, J., Moman, E., Roessle, M., Peluso-Iltis, C., Moulin, M., Haertlein, M., Callow, P., Mély, Y., et al. (2011). Common architecture of nuclear receptor heterodimers on DNA direct repeat elements with different spacings. Nat. Struct. Mol. Biol. *18*, 564–570. https://doi.org/10.1038/nsmb.2054.

Rogatsky, I., Zarember, K.A., and Yamamoto, K.R. (2001). Factor recruitment and TIF2/GRIP1 corepressor activity at a collagenase-3 response element that mediates regulation by phorbol esters and hormones. EMBO J. *20*, 6071–6083. https://doi.org/10.1093/emboj/20.21.6071.

Ross, A.C., and Zolfaghari, R. (2011). Cytochrome P450s in the regulation of cellular retinoic acid metabolism. Annu. Rev. Nutr. *31*, 65–87. https://doi.org/10.1146/annurev-nutr-072610-145127.

Schug, T.T., Berry, D.C., Shaw, N.S., Travis, S.N., and Noy, N. (2007). Opposing effects of retinoic acid on cell growth result from alternate activation of two different nuclear receptors. Cell *129*, 723–733. https://doi.org/10.1016/j.cell.2007.02.050.

Schwarz, E.J., Reginato, M.J., Shao, D., Krakow, S.L., and Lazar, M.A. (1997). Retinoic acid blocks adipogenesis by inhibiting C/EBPbeta-mediated transcription. Mol. Cell Biol. *17*, 1552–1561. https://doi.org/10.1128/MCB.17.3.1552.

Senicourt, L., le Maire, A., Allemand, F., Carvalho, J.E., Guee, L., Germain, P., Schubert, M., Bernadó, P., Bourguet, W., and Sibille, N. (2021). Structural insights into the interaction of the intrinsically Disordered Co-activator TIF2 with retinoic acid receptor heterodimer (RXR/RAR). J. Mol. Biol. *433*, 166899. https://doi.org/10.1016/j.jmb.2021.166899.

Surjit, M., Ganti, K.P., Mukherji, A., Ye, T., Hua, G., Metzger, D., Li, M., and Chambon, P. (2011). Widespread negative response elements mediate direct repression by agonist- liganded glucocorticoid receptor. Cell *145*, 224–241. https://doi.org/10.1016/j.cell.2011.03.027.

Tay, S., Dickmann, L., Dixit, V., and Isoherranen, N. (2010). A comparison of the roles of peroxisome proliferator-activated receptor and retinoic acid receptor on CYP26 regulation. Mol. Pharmacol. *77*, 218. https://doi.org/10.1124/mol.109.059071.

Teslovich, T.M., Musunuru, K., Smith, A.V., Edmondson, A.C., Stylianou, I.M., Koseki, M., Pirruccello, J.P., Ripatti, S., Chasman, D.I., Willer, C.J., et al. (2010). Biological, clinical and population relevance of 95 loci for blood lipids. Nature *466*, 707–713. https://doi.org/10.1038/nature09270.

Thatcher, J.E., and Isoherranen, N. (2009). The role of CYP26 enzymes in retinoic acid clearance. Expert Opin. Drug Metab. Toxicol. *5*, 875–886. https://doi.org/10.1517/17425250903032681.

Trasino, S.E., Benoit, Y.D., and Gudas, L.J. (2015). Vitamin a deficiency causes hyperglycemia and loss of pancreatic β-cell mass. J. Biol. Chem. *290*, 1456–1473. https://doi.org/10.1074/jbc.M114.616763.

Trasino, S.E., Tang, X.-H., Jessurun, J., and Gudas, L.J. (2016). Retinoic acid receptor β2 agonists restore glycaemic control in diabetes and reduce steatosis. Diabetes Obes. Metab. *18*, 142–151. https://doi.org/10.1111/dom.12590.

Tuteja, S., Qu, L., Vujkovic, M., Dunbar, R.L., Chen, J., DerOhannessian, S., and Rader, D.J. (2018). Genetic variants associated with plasma lipids are associated with the lipid response to Niacin. J. Am. Heart Assoc. *7*, e03488. https://doi.org/10.1161/JAHA.117.008461.

Vakharia, K., and Hinson, J.P. (2005). Lipopolysaccharide directly stimulates cortisol secretion by human adrenal cells by a cyclooxygenase-dependent mechanism. Endocrinology *146*, 1398–1402. https://doi.org/10.1210/en.2004-0882.

Wang, T., Ma, X., Krausz, K.W., Idle, J.R., and Gonzalez, F.J. (2008). Role of pregnane X receptor in control of all-trans retinoic acid (ATRA) metabolism and its potential contribution to ATRA resistance. J. Pharmacol. Exp. Ther. *324*, 674–684. https://doi.org/10.1124/jpet.107.131045.

Wang, X., Sperkova, Z., and Napoli, J.L. (2001). Analysis of mouse retinal dehydrogenase type 2 promoter and expression. Genomics *74*, 245–250. https://doi.org/10.1006/geno.2001.6546.

White, J.A., Guo, Y.D., Baetz, K., Beckett-Jones, B., Bonasoro, J., Hsu, K.E., Dilworth, F.J., Jones, G., and Petkovich, M. (1996). Identification of the retinoic acid-inducible all-trans-retinoic acid 4-hydroxylase. J. Biol. Chem. *271*, 29922–29927. https://doi.org/10.1074/jbc.271.47.29922.

Wolf, G. (2001). Retinoic acid homeostasis: retinoic acid regulates liver retinol esterification as well as its own catabolic oxidation in liver. Nutr. Rev. *59*, 391–394. https://doi.org/10.1111/j.1753-4887.2001.tb06968.x.

Wołoszynowska-Fraser, M.U., Kouchmeshky, A., and McCaffery, P. (2020). Vitamin A and retinoic acid in cognition and cognitive disease. Annu. Rev. Nutr. *40*, 247–272. https://doi.org/10.1146/annurev-nutr-122319-034227.

Yamamoto, Y., Zolfaghari, R., and Ross, A.C. (2000). Regulation of CYP26 (cytochrome P450RAI) mRNA expression and retinoic acid metabolism by retinoids and dietary vitamin A in liver of mice and rats. FASEB J. *14*, 2119–2127. https://doi.org/10.1096/fj.00-0061com.

Yang, D., Vuckovic, M.G., Smullin, C.P., Kim, M., Lo, C.P.-S., Devericks, E., Yoo, H.S., Tintcheva, M., Deng, Y., and Napoli, J.L. (2018). Modest decreases in endogenous all-trans-retinoic acid produced by a mouse rdh10 heterozygote provoke major abnormalities in adipogenesis and lipid metabolism. Diabetes *67*, 662–673. https://doi.org/10.2337/db17-0946.

Zhang, M., Hu, P., Krois, C.R., Kane, M.A., and Napoli, J.L. (2007). Altered vitamin A homeostasis and increased size and adiposity in the rdh1-null mouse. FASEB J. *21*, 2886–2896. https://doi.org/10.1096/fj.06-7964com.

Zhang, Y., Zolfaghari, R., and Ross, A.C. (2010). Multiple retinoic acid response elements cooperate to enhance the inducibility of CYP26A1 gene expression in liver. Gene *464*, 32–43. https://doi.org/10.1016/j.gene.2010.05.004.

Zhao, Y., Vuckovic, M., Yoo, H.S., Fox, N., Rodriguez, A., McKessy, K., and Napoli, J.L. (2021). Retinoic acid exerts sexually dimorphic effects on muscle energy metabolism and function. J. Biol. Chem. *297*, 101101. https://doi.org/10.1016/j.jbc.2021.101101.

Zhong, G., Hogarth, C., Snyder, J.M., Palau, L., Topping, T., Huang, W., Czuba, L.C., LaFrance, J., Ghiaur, G., and Isoherranen, N. (2019). The retinoic acid hydroxylase Cyp26a1 has minor effects on postnatal vitamin A homeostasis, but is required for exogenous atRA clearance. J. Biol. Chem. *294*, 11166–11179. https://doi.org/10.1074/jbc.RA119.009023.

Zolfaghari, R., Cifelli, C.J., Lieu, S.O., Chen, Q., Li, N., and Ross, A.C. (2007). Lipopolysaccharide opposes the induction of CYP26A1 and CYP26B1 gene expression by retinoic acid in the rat liver in vivo. Am. J. Physiol. Gastrointest. Liver Physiol. *292*, G1029–G1036. https://doi.org/10.1152/ajpgi.00494.2006.

Zolfaghari, R., and Ross, A.C. (2000). Lecithin:retinol acyltransferase from mouse and rat liver. CDNA cloning and liver-specific regulation by dietary vitamin a and retinoic acid. J. Lipid Res. *41*, 2024–2034.

STAR★METHODS

KEY RESOURCES TABLE

REAGENT or RESOURCE	SOURCE	IDENTIFIER
Antibodies		
Rabbit polyclonal anti-IgG	Abcam	Cat# ab2410; RRID AB_303052
Rabbit monoclonal anti-GR	Cell Signaling Technology	Cat# 12041; RRID: AB_2631286
Rabbit monoclonal anti-RARα	Cell Signaling Technology	Cat# 62294; RRID: AB_2799625
Rabbit monoclonal anti-RARγ	Cell Signaling Technology	Cat# 8965; RRID: AB_10998934
Rabbit polyclonal anti-C/EBPβ	Cell Signaling Technology	Cat# 90081; RRID: AB_2078052
Bacterial and virus strains		
Subcloning Efficiency™ DH5α Competent Cells	ThermoFisher	Cat# 18265017
Biological samples		
Human: Cryopreserved pooled plateable human hepatocytes	ThermoFisher	Cat# HMCPP5
Critical commercial assays		
Dual-Luciferase Reporter Assay System	Promega	Cat# E1910
QuikChange XL Site-Directed Mutagenesis Kit	Agilent	Cat# 200516
Lipofectamine 3000	ThermoFisher	Cat# L3000008
Experimental models: Cell lines		
Human: HepG2	Cell Culture Facility at University of California, Berkeley	N/A
Human: HeLa	Cell Culture Facility at University of California, Berkeley	N/A
Experimental models: Organisms/strains		
Mouse: C57BL/6J	The Jackson Laboratory	JAX: 000664
Oligonucleotides		
siRNA-negative control	ThermoFisher	Cat# 4390843
siRNA-CEBPB	ThermoFisher	Cat# 4392420
ss oligo DNA (5′-GGACTCACTCTGGAAAATGA CCCTTCGGGCTCCTAGCAGCATGGTGTAGCA ATAGTGGTGCTGTGCTGTCCAGGGCTGCTGC GGGTGGGCGACCAAGCTGG-3′)	This paper	N/A
Recombinant DNA		
pGL4.10[luc2] Promoterless Firefly Luciferase Basic Vector	Promega	Cat# E6651
pGL4.73[hRluc/SV40] control vector	Promega	Cat# E6911
Software and algorithms		
GraphPad Prism 7		

RESOURCE AVAILABILITY

Lead contact

Further information and requests for resources and reagents should be directed to and will be fulfilled by the lead contact, Joseph L. Napoli (jna@berkeley.edu).

Materials availability

- Plasmids generated in this study will be made available upon request to the Lead contact.
- Edited HeLa cells generated in this study will be made available upon request to the Lead contact.

Data and code availability

- All dataset generated or analyzed during this study are included in the published article. Detailed datasets supporting the current study are available from the Lead contact upon request.
- This paper does not report original code.
- Any additional information required to reanalyze the data reported in this paper is available from the Lead contact upon request.

EXPERIMENTAL MODEL AND SUBJECT DETAILS

Animal experiments

C57BL/6J (000664) male and female mice were purchased from The Jackson Laboratory and bred >3 generations fed a purified AIN93G diet containing 4 IU vitamin A/g (Research Diets, D10012G), because copious vitamin A affects experimental models (Obrochta et al., 2014). Littermates of the same sex were randomly assigned to experimental groups (8-12 weeks old). Liver samples were collected from mice fasted 16 hr and compared to those refed 6 h after a 16 h fast, following anesthesia in an isoflurane chamber. Tissues were snap-frozen in liquid nitrogen and stored at −80°C until assay. Animal experiment protocols were approved by the University of California Berkeley Animal Care and Use Committee.

Cell culture

HepG2 and HeLa cells were obtained from the Cell Culture Facility, University of California, Berkeley and maintained in EMEM (ATCC, 30-2003), supplemented with 10% heat-inactivated fetal bovine serum (FBS) (Gibco, 10082) at 37°C under 5% CO_2. Cells were cultured no >20 passages. To minimize effects of unknown factors, growth medium was replaced with serum-free medium and incubated 18 h prior to experiments. Cryopreserved pooled plateable human hepatocytes (ThermoFisher, HMCPP5) were purchased and seeded on a 12-well plate in William's E medium (ThermoFisher, A1217601) and primary hepatocyte thawing and plating supplements (ThermoFisher, CM3000), following manufacturer's instructions, and then incubated 12 h at 37°C under 5% CO_2. The medium was replaced with William's E medium and primary hepatocyte maintenance supplements (ThermoFisher, CM4000) and incubated 2 h, followed by the experimental protocol.

METHOD DETAILS

Gene expression assays

Total RNA was isolated using TRI Reagent (Sigma, T9424), quantified using NanoDrop One (ThermoFisher), and reverse-transcribed using iScript cDNA Synthesis Kit (Bio-Rad, 1708891. qPCR was performed with a Bio-Rad CFX Connect Real-Time Detection System using PrimeTime Gene Expression Master Mix (Integrated DNA Technologies (IDT), 1055772). Gene expression was analyzed by the $\Delta\Delta$-Ct method, normalized to *GusB* and expressed as fold change relative to controls. Primers used were: *GUSB* (IDT, Hs.PT.58v.27737538), *Gusb* (IDT, Mm.PT.39a.22214848), *CYP26A1* (IDT, Hs.PT.58.2905296), *Cyp26a1* (IDT, Mm.PT.58.10791878) and *CEBPB* (ThermoFisher, Hs00270923_s1).

Quantification of RA in tissues and cells

RA was quantified by LC-MS/MS, following a published method with the modification that homogenates were centrifuged 5 min at 1,200 × g to remove precipitates (Kane et al., 2008). LC was modified as published (Arnold et al., 2012).

To measure the RA elimination t½, HepG2 (7×10^5 cells) were seeded on 6-well plates in EMEM +10% FBS. After 24 h, cells were FBS-starved for 18 h, then treated with 100 nM RA ± 100 nM Dex for 3 h. The medium was removed, and cells were rinsed with 1 mL PBS. Cells were collected by adding 1 mL of passive lysis buffer (Promega, E194) at 0, 2, 3, 6, 8 h. A Bradford assay quantified protein in 50 µL cell lysate. The remaining material was mixed with 2 mL methanol to extract and quantify RA as described above.

Cloning reporter vectors

Inserts of constructs a, b and c were prepared by PCR amplification of *CYP26A1* promoter regions using primers listed in Table S1 and DNA isolated from HepG2 cells. Amplified DNA fragments were isolated by gel electrophoresis and digested with restriction enzymes, KpnI (NEB, R0142), HindIII (NEB, R0104),

BglII (NEB, R0144) or NheI (NEB, R0131) and ligated into the pGL4.10[luc2] Promoterless Firefly Luciferase Basic Vector (Promega, E6651). Subcloning Efficiency™ DH5α Competent Cells (ThermoFisher, 18265017) were transformed with the ligated products and plated onto LB agar including 100 μg/mL ampicillin. After incubation overnight at 37°C, five CFUs were placed into LB Broth/ampicillin and incubated overnight at 37°C. Vectors were isolated using Plasmid Maxi Kit (Qiagen, 12,162). Sequences were confirmed by DNA sequencing.

Transfection and luciferase assay

HepG2 cells were seeded onto 24-well plates with EMEM and 10% FBS at 60-70% confluence. After 24 h incubation, the medium was replaced with EMEM with 10% charcoal-stripped FBS (ThermoFisher, A3382101). Cells were transfected with 100 ng/well reporter vector and 10 ng/well control vector, pGL4.73[hRluc/SV40] (Promega, E6911) using Lipofectamine 3000 (ThermoFisher, L3000008), followed by 24 h incubation. The medium was replaced with FBS-free EMEM. Cells were treated 6 h with 0.1% DMSO or 1 μM RA ± 1 μM Dex. Cells were washed with 500 μL PBS (pH 7.4) and lysed with 120 μL passive lysis buffer (Promega, #E194A). Luminescence was measured with a mix of 20 μL cell lysate and 75 μL substrate in a 96-well plate using the Dual-Luciferase Reporter Assay System (Promega, E1910) and a SpectraMax i3 plate reader (Molecular Devices).

ChIP-qPCR

HepG2 cells, seeded onto 15 cm dishes, were treated 30 min with 0.1% DMSO, 1 nM RA, 100 nM Dex or both. Cross-linking was done 10 min with 1% formaldehyde at room temperature. The reaction was quenched by addition of 125 mM glycine. Cells were rinsed with 10 mL ice-cold PBS plus protease inhibitor (ThermoFisher, A32963). After addition of 5 mL ice-cold PBS plus protease inhibitor, cells were collected into a 15 mL conical tube, centrifuged 3 min at 500 × g at 4°C. Supernatant was removed. One mL cold RIPA buffer (ThermoFisher, 89900) and protease inhibitor were applied to lyse the pellet, then sheared 17 min using Covaris S220 Focused-ultrasonicator at PIP 140, DF 5, CBP 200 at 4°C. Samples were centrifuged 10 min at 15,000 × g at 4°C. The sheared chromatin sample was divided for immunoprecipitation—20 μL for input and 150 μL for immunoprecipitation; 26.2 μL IgG Ab (Abcam, ab2410), 2 μL GR Ab (Cell Signaling Technology, 12041), 2 μL RARα Ab (Cell Signaling Technology, 62294), 2 μL RARγ1 Ab (Cell Signaling Technology, 8965), 2 μL C/EBPβ Ab (Cell Signaling Technology, 90081). Thirty μL protein A/G plus-agarose bead (Santa Cruz Biotechnology, sc-2003), prepared in 1 mL RIPA buffer and 10 μL salmon sperm DNA (Abcam ab229278), were added. Samples were rotated 2 h at 4°C. 500 μL washes were done: twice with RIPA; twice with RIPA and NaCl adjusted to 500 mM; twice with LiCl buffer (20 mM Tris-HCl at pH 8.0, 1 mM EDTA, 250 mM LiCl, 0.5% NP-40, and 0.5% sodium deoxycholate), once with RIPA. To reverse cross-linking, 74 μL TE/SDS buffer (10 mM Tris-Cl (pH 8.0), 1 mM EDTA, 0.9% SDS) and 1 μL of 20 mg/mL protease K were added to each sample. Samples were incubated 3 h at 55°C, then 3 M NaCl (6.6 μL) and 10 mg/mL RNase A (1 μL) were added and incubated overnight at 65°C. DNA was extracted with a QIAquick PCR Purification Kit (Qiagen, 28104). Real-time qPCR was done for analysis. Primers are listed in Table S2.

Co-immunoprecipitation and western blotting

HepG2 cells were treated 30 min with 0.1% DMSO, 1 nM RA, 100 nM dexamethasone or both, then cross-linked 30 min with 3 mM disuccinimidyl glutarate (ThermoFisher, 20593), followed by 15 min quenching with 30 mM glycine. Cells were rinsed with 10 mL ice-cold PBS plus protease inhibitor (ThermoFisher, A32963). After addition of 5 mL ice-cold PBS plus the protease inhibitor, cells were collected into a 15 mL conical tube, centrifuged 3 min 500 × g at 4°C, followed by removal of supernatant. One mL RIPA buffer (ThermoFisher, 89900) and the protease inhibitor were added to lyse the pellet. Cell lysates were centrifuged 10 min at 15,000 × g at 4°C. Two hundred μL supernatant were collected, mixed with 2 μL of RARα Ab and mixed overnight at 4°C. Thirty μL of protein A/G plus-agarose beads were added. Samples were mixed 2 h at 4°C. 500 μL washes were done: 5 times with RIPA; once with PBS. After removing supernatant, 30 μL of Laemmli sample buffer (Bio-Rad, 1610737) including 5% β-mercaptoethanol were added. Samples were heated 5 min at 95°C and cooled on ice.

Proteins were separated by 7.5% SDS-PAGE (Bio-Rad, 4561024), transferred onto nitrocellulose membranes (Bio-Rad, 1620115), and immunoblotted overnight at 4°C with antibodies against GR, RARα and β-actin (Abcam, ab8226). Primary antibodies were diluted 1: 2,000. Near-infrared fluorescent

dye-conjugated secondary antibodies were: anti-rabbit (LI-COR, 926-32211) and anti-mouse (LI-COR, 926-68070) at 1: 5,000. Immunoblots were developed with an Odyssey Imaging System (LI-COR).

Site-directed mutagenesis

Site-directed mutagenesis was done using the QuikChange XL Site-Directed Mutagenesis Kit (Agilent, 200516).

CEBPB knock down

HepG2 cells were seeded onto a 12-well plate with EMEM supplemented with 10% FBS at 60-70% confluence. After 24 h incubation, cells were transfected with 5 pmol siRNA-negative control (ThermoFisher, 4390843) or 5 pmol siRNA-*CEBPB* (ThermoFisher, 4392420) using Lipofectamine 3000 then incubated 12 h. Cells were FBS-starved 2 h before treatment with 1 nM RA. *CEBPB* and *CYP26A1* mRNAs were measured by the gene expression assay protocol.

CRISPR/Cas9-mediated single 'base edit

SNP rs2068888 minor allele was generated in HeLa cells using the CRISPR/Cas9 system, following Cas9/sgRNA manufacturer's instruction. Cells were seeded onto a 24-well plate and were transfected at 60-70% confluence. Prior to transfection, Cas9 ribonucleoproteins (RNPs) were generated with 25 μL.

Opti-MEM™ medium, 1250 ng (7.5 pmol) TrueCut™ Cas9 Protein v2 (ThermoFisher, A36496), 240 ng (7.5 pmol) sgRNA (5′-TAGCAGCATGGTGTAGCGAT-3′) and 2.5 μL Cas9 Plus™ Reagent (all amounts are provided for a single well). The mixture was incubated 5 min to allow formation of Cas9 RNPs. Five hundred ng of the ss oligo DNA (5′- GGACTCACTCTGGAAAATGACCCTTCGGGCTCCTAGCAGCATGGTGTAGC AATAGTGGTGCT GTGCTGTCCAGGGCTGCTGCGGGTGGGCGACCAAGCTGG-3′) were added to the Cas9 RNPs in each well. A Lipofectamine™ CRISPRMAX™ tube was prepared with 25 μL of Opti-MEM medium and 1.5 μL of Lipofectamine™ CRISPRMAX™ (ThermoFisher, CMAX00001). This solution was incubated 2 min. Cas9 RNPs were added and incubated 15 min at room temperature. Fifty μL of the transfection complex were added to each well. Cells were incubated 48 h at 37°C.

DNA sequencing

The region of DNA sequenced was amplified by PCR with forward primer 5′- ATGTTTTATGG CACAGTCAC-3′ and reverse primer 5′-ACAGTCCTGATTGAAGAGAAC-3′. PCR amplification was done with Taq DNA Polymerase with 1,000 ng of genomic DNA as template (New England BioLabs, M0273S). After PCR, 2% agarose gel electrophoresis was done to visualize products, which were extracted using the Monarch® DNA Gel Extraction Kit (New England BioLabs, T1020S). Isolated DNA was sequenced by the UC Berkeley DNA Sequencing Facility with the PCR forward primer as sequencing primer.

QUANTIFICATION AND STATISTICAL ANALYSIS

Data are means ± SEM. Two-tailed unpaired t-tests compared data between two groups. Two-way ANOVA was used as noted. Statistical testing was done using GraphPad Prism 7 (San Diego, CA).